Mixed-Feedback Architectures for Precise Event Timing Through Stochastic Accumulation of Biomolecules

Sayeh Rezaee[1], César Nieto[2], and Abhyudai Singh[3]

***Abstract*— The timing of biochemical events is often determined by the accumulation of a protein or chemical species to a critical threshold level. In a stochastic model, we define event timing as the first-passage time for the level to cross the threshold from zero or random initial conditions. This first-passage time can be modulated by implementing feedback in synthesis, that is, making the production rate an arbitrary function of the current species level. We aim to find the optimal feedback strategy that reduces the timing noise around a given mean first-passage time. Previous results have shown that while a no-feedback strategy (i.e., an independent constant production rate) is optimal in the absence of degradation and zero-molecules initial condition, a negative feedback is optimal when the process starts at random initial conditions. We show that when the species can be degraded and the synthesis rates are set to depend linearly on the number of molecules, a positive feedback strategy (the production rate increases with the level of the molecule) minimizes timing noise. However, if no constraints on the feedback are imposed, the optimal strategy involves a mixed feedback approach, which consists of an initial positive feedback followed by a sharp negative feedback (the production rate decreases with the level) near the threshold. Finally, we quantify the fundamental limits of timing noise reduction with and without feedback control when time-keeping species are subject to degradation.**

I. Introduction

Precision in the timing of biochemical events within cells is needed for high fidelity functioning despite inherently noisy processes occurring with low-copy number components. Several biological processes critically depend on timing mechanisms based on threshold-crossing of given variables. These include, neuronal firing of action potential, cell-cycle regulation, tissue development, biological clocks, apoptosis, signal transduction, and gene activation [1]–[12]. This time variability can be reduced by using self-regulation in protein synthesis rates [13]–[17]. Self-regulation strategies, also known as feedback, involve adjusting the transcription/translation rate based on the current protein level. Finding an optimal feedback technique that minimizes this timing variability in particular systems is crucial to understanding the mechanisms of cell timing, and uncovering the fundamental limits of timing noise suppression.

One of the most used approaches for modeling cell timing is based on first-passage time (FPT) statistics [18]–[25]. Different feedback regulation schemes have been explored, and different parameters have been optimized to minimize the FPT variability while keeping the mean FPT constant [13]–[17], [26]. The solution for simple systems such as constant protein production without degradation or dilution has already been studied. Interestingly, for this system, the minimum timing noise is achieved if there is no feedback [27]. Recently, we have shown that if the protein is continuously diluted, the effect of dilution can be compensated by a feedback strategy that increases the transcription rate as the protein level increases [28]. However, this model has some limitations. First, it assumes that dilution is a continuous deterministic process, but for some biochemical systems, stochastic protein degradation may be more relevant than dilution. Second, it assumes that the feedback strategy is linearly dependent on the protein level. In a general approach, the optimal feedback strategy is expected not to grow linearly with the protein amount but to be an arbitrary function of this number. To date, the general solution to this problem of optimization characterizing timing accuracy is unknown.

In this study, we address the limitations mentioned above. Specifically, we employ a modeling framework wherein protein levels are represented as discrete random variables. Moreover, protein production and degradation mechanisms are characterized as stochastic birth-death processes. The occurrence rates of these processes depend on the protein level, such that the degradation probability of a protein molecule increases linearly with the protein copy number, and the synthesis rate is an arbitrary function of this number. Our primary objective is to investigate the feedback function that minimizes noise in FPT around a predetermined fixed mean.

The article consists of the following sections: First, we review the problem and the solution in the absence of degradation with both zero-molecule initial conditions and a random initial protein number. Second, we consider optimizing the slope of a linear synthesis rate with stochastic degradation. We use the small-noise approximation to obtain analytic formulas that are valid for high threshold numbers. Third, we present a solution for the low-number regime. We analytically solve the optimization problem for two molecules and numerically solve the master equation of the system for five molecules, optimizing over the synthesis rates to minimize FPT fluctuations. As a main result, mixed feedback emerges as optimal, wherein the synthesis rate increases non monotonically with the protein level and sharply declines near the threshold. Finally, we discuss the implications of our findings for biological systems and suggest potential

[1],[2]Department of Electrical and Computer Engineering, University of Delaware, Newark, DE, USA {sayehr, cnieto}@udel.edu

[3]Department of Electrical and Computer Engineering, Biomedical Engineering, Mathematical Sciences, Center of Bioinformatic and Computational Biology, University of Delaware, Newark, DE, USA {absingh}@udel.edu

applications.

II. Formulating event timing as a first-passage time problem

Let $x(t) \in \{0, 1, 2, \dots\}$ be an integer-valued process representing the molecular count of a certain biochemical species at time t. The time evolution of $x(t)$ can be modeled as a birth-death process with a constant synthesis rate k and a degradation rate γ. More specifically, synthesis events occur according to a Poisson process with rate k. In this case, the probability of copy numbers increasing from i to $i+1$ in an infinitesimal time interval $(t, t+dt]$ is given by:

$$\mathbb{P}\{x(t+dt) = i+1 | x(t) = i\} = kdt. \tag{1}$$

The timespan each molecule lives is an independent and identically distributed random variable that is exponentially distributed with mean timespan $1/\gamma$, and corresponds to the following probability of degradation:

$$\mathbb{P}\{x(t+dt) = i-1 | x(t) = i\} = \gamma i dt. \tag{2}$$

A feedback loop is implemented by allowing the production rate k_i, to vary arbitrarily with the current levels of the species, denoted as $x(t) = i$. This alters the synthesis probability (1) to

$$\mathbb{P}\{x(t+dt) = i+1 | x(t) = i\} = k_i dt, \quad i \in \{0, 1, 2, \dots\}, \tag{3}$$

where the time required for transition from i to $i+1$ molecules is exponentially distributed with mean $1/k_i$. This formalism enables the realization of various feedback scenarios:

- A constant synthesis rate $k_i = k$ corresponds to a no-feedback strategy.
- Negative feedback corresponds to k_i decreasing with increasing i, i.e., the synthesis rate declines with higher molecular counts.
- Similarly, positive feedback corresponds to k_i increasing with i.
- Nonmonotonic shapes of k_i capture complex feedback strategies that combine both negative and positive feedbacks.

Let a positive integer X be a critical threshold level for molecular counts that triggers an event. Then, event timing is a random variable defined by the first-passage time (FPT)

$$T := \inf\{t \geq 0 : x(t) \geq X | x(0) = x_0 < X\}, \tag{4}$$

which corresponds to the first time the random process $x(t)$ reaches X starting from an initial condition x_0 at time $t = 0$. For a fixed X and degradation rate γ, our goal is to determine the optimal feedback strategy $k_i, i \in \{0, 1, 2, \dots X-1\}$ for synthesizing molecules that minimizes the random fluctuations in T, *while ensuring a given mean first-passage time* (Fig. 1B).

III. Optimal feedback strategy in the absence of degradation

Having formulated the problem, we first focus on the special case of no degradation i.e., $\gamma = 0$, where molecular counts only build up over time.

A. FPT problem with Zero-molecules initial condition

If the system starts with zero molecules with probability one at $t = 0$, the first-passage time is essentially a sum of each reaction time, which is an exponentially distributed random variable with mean $1/k_i$, $i \in \{0, 1, \dots, X-1\}$. Using the angular brackets $\langle\ \rangle$ to denote the expected-value operation, the moments of T follow

$$\langle T \rangle = \sum_{i=0}^{X-1} \frac{1}{k_i}, \quad \langle T^2 \rangle = \left(\sum_{i=0}^{X-1} \frac{1}{k_i} \right)^2 + \sum_{i=0}^{X-1} \frac{1}{k_i^2}, \tag{5}$$

which leads to the variance as below.

$$\sigma_T^2 := \langle T^2 \rangle - \langle T \rangle^2 = \sum_{i=0}^{X-1} \frac{1}{k_i^2}. \tag{6}$$

Our goal is to find the optimal sequence k_i, $i \in \{0, 1, \dots, X-1\}$ that minimizes the variance σ_T^2 while keeping $\langle T \rangle$ fixed. To obtain the solution, we propose that optimal rates can be written as

$$k_i := \frac{1}{\frac{\langle T \rangle}{X} + \epsilon_i}, \tag{7}$$

with $\epsilon_i \in \mathbb{R}$ having arbitrary values. If we fix $\langle T \rangle$ from (5), the following constraint

$$\sum_{i=0}^{X-1} \epsilon_i = 0 \tag{8}$$

is required to ensure a fixed mean FPT. On the other hand, using (6) and (8), the variance in FPT is given by

$$\begin{aligned} \sigma_T^2 = \sum_{i=0}^{X-1} \frac{1}{k_i^2} &= \sum_{i=0}^{X-1} \left(\frac{\langle T \rangle}{X} + \epsilon_i \right)^2 \\ &= \frac{\langle T \rangle^2}{X} + \frac{2\langle T \rangle}{X} \sum_{i=0}^{X-1} \epsilon_i + \sum_{i=0}^{X-1} \epsilon_i^2 \\ &= \frac{\langle T \rangle^2}{X} + \sum_{i=0}^{X-1} \epsilon_i^2 \end{aligned} \tag{9}$$

The sum of squares ϵ_i^2 on the right-hand-side of (9) is minimized only when all $\epsilon_i = 0$. Therefore, the optimal feedback strategy is to set a constant synthesis rate as:

$$k_i = \frac{X}{\langle T \rangle} \quad i \in \{0, 1, \dots, X-1\} \tag{10}$$

and the corresponding optimal noise in FPT

$$CV_T^2 := \frac{\sigma_T^2}{\langle T \rangle^2} = \frac{1}{X} \tag{11}$$

as quantified by its coefficient of variation.

In summary, when $\gamma = 0$, to reach a threshold at a prescribed time, *the optimal strategy is to have a constant synthesis rate, and any form of feedback will amplify timing fluctuations* [27]. Moreover, $1/X$, the inverse of the threshold level, is the fundamental limit to which timing noise can be suppressed. Previous studies have extended this problem to consider production occurring in molecular bursts, as seen

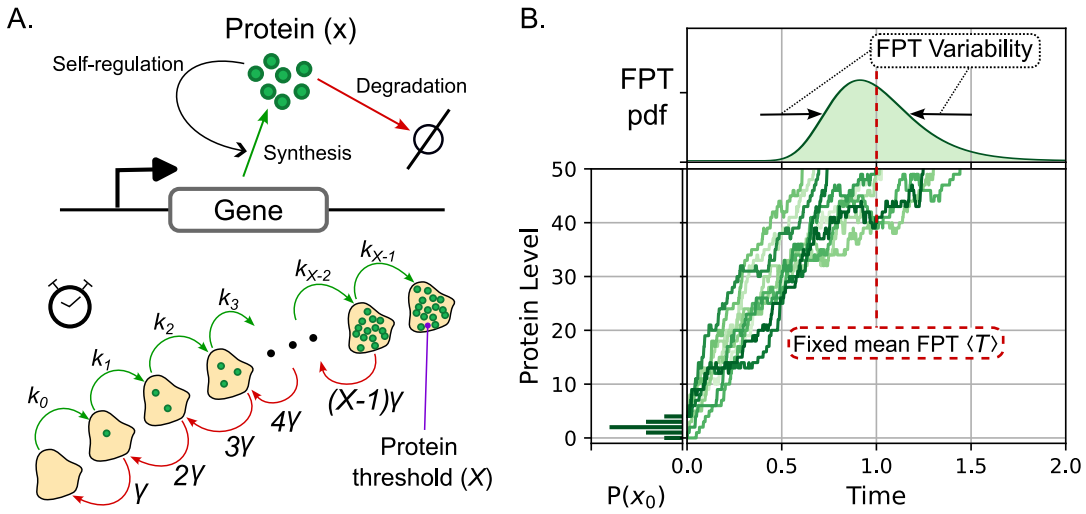

Fig. 1: **Event timing of biochemical processes triggered by the accumulation of proteins to a threshold**. **A.** Model of protein synthesis and degradation from gene expression. Feedback is implemented by allowing the synthesis rate k_i to vary as a function of the current protein level. The stochastic dynamics of the protein count is modeled as a birth-death process. Synthesis, wherein the number of molecules jumps from i to $i+1$, occurs at a rate k_i. Additionally, the degradation, which is the jump from i to $i-1$, occurs at a rate γi. **B.** Example trajectories of protein copy number over time starting from a random initial condition. The event is triggered when the level reaches a critical threshold. Our goal is to obtain the strategy of k_i that minimizes the stochastic variability in the FPT. In the optimization, we fix the threshold X, the degradation rate γ, and the average time $\langle T\rangle$ required to reach the threshold.

in gene expression measurement in single cells [29]–[36], that is, each synthesis event produces several molecules in contrast to just one molecule as considered here. For this bursty-birth process, the optimal feedback in the absence of degradation is similar to a no-feedback strategy, where all k_i, $i \in \{1,\dots,X-1\}$ are exactly the same except for the first synthesis rate k_0 that is lower than the rest [27], [37], [38].

B. Random initial condition

We next extend the mentioned results to consider the process starting with a random initial condition as follows.

$$\mathbb{P}\{x(0)=i\}=p_i,\ i\in\{0,1,\dots,X-1\}. \tag{12}$$

This assumption leads to the following mean FPT,

$$\begin{aligned}\langle T\rangle &= \sum_{i=0}^{X-1} p_i\langle T|x(0)=i\rangle \\ &= \sum_{i=0}^{X-1} p_i \sum_{j=i}^{X-1}\frac{1}{k_j} \\ &= \frac{p_0}{k_0}+\frac{p_0+p_1}{k_1}+\frac{p_0+p_1+p_2}{k_2}+\ldots+\frac{1}{k_{X-1}},\end{aligned} \tag{13}$$

and its corresponding (uncentered) second-order moment.

$$\langle T^2\rangle = \sum_{i=0}^{X-1} p_i\langle T^2|x(0)=i\rangle, \tag{14}$$

where

$$\langle T^2|x(0)=i\rangle = \left(\sum_{j=i}^{X-1}\frac{1}{k_j}\right)^2+\sum_{j=i}^{X-1}\frac{1}{k_j^2}. \tag{15}$$

To perform the optimization, one can find k_0 as a function of $k_1,\dots,k_{X-1}$ from (13) to have a fixed $\langle T\rangle$. Substituting this value of k_0 into (14), one can then optimize over $k_1,\dots,k_{X-1}$ to minimize $\langle T^2\rangle$. We did the optimization by simultaneously solving the equations

$$\frac{d\langle T^2\rangle}{dk_i}=0,\ i\in\{1,\dots,X-1\} \tag{16}$$

to find the rates $k_1,\dots,k_{X-1}$.

We illustrate the results for a threshold of $X=6$ molecules. If the initial condition is zero molecules with probability p_0 and one molecule with probability $1-p_0$ then the optimal rates are

$$\begin{aligned}k_0 &= \frac{10-4p_0}{\langle T\rangle} \\ k_i &= \frac{10-4p_0}{(2-p_0)\langle T\rangle},\ i\in\{1,\dots,X-1\},\end{aligned} \tag{17}$$

where all $k_i, i\in\{1,\dots,X-1\}$ are equal and k_0 set higher than the rest. As anticipated, when $p_0\to 1$, the result converges to having all rates as $6/\langle T\rangle$. In addition, if we consider an initial condition with equal probability in all states, meaning $p_i=1/6,\ i\in\{0,1,\dots,X-1\}$, then the optimal rates are

$$\begin{aligned}k_0 &= \frac{12.88}{\langle T\rangle},\ k_1=\frac{8.59}{\langle T\rangle},\ k_2=\frac{5.95}{\langle T\rangle}, \\ k_3 &= \frac{4.24}{\langle T\rangle},\ k_4=\frac{3.08}{\langle T\rangle},\ k_5=\frac{2.29}{\langle T\rangle}.\end{aligned} \tag{18}$$

which corresponds to a negative feedback strategy with rates decreasing as i increases.

In the next section, we describe the optimization problem in the presence of protein degradation assuming a linear synthesis rate and a low-noise limit with a large threshold X.

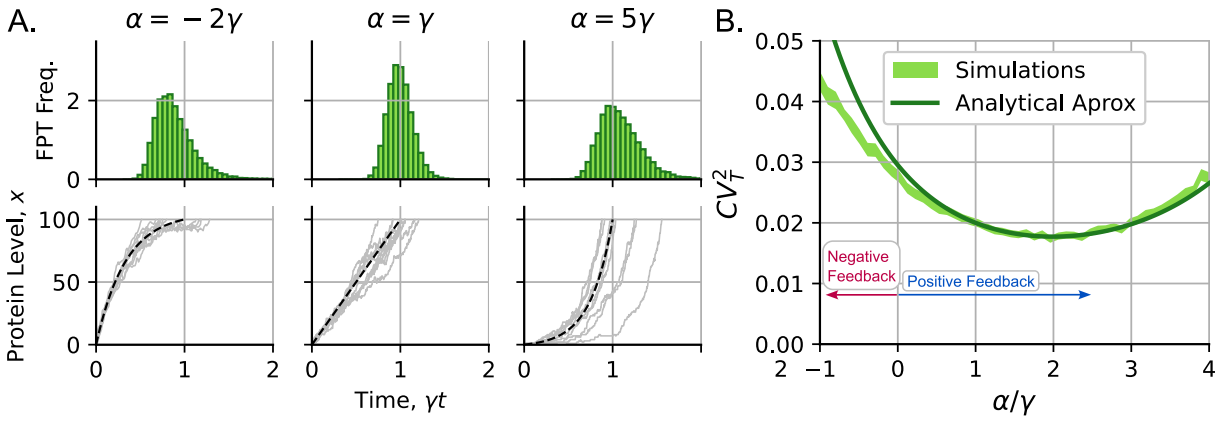

Fig. 2: **Stochasticity in FPT for linear protein synthesis rates and spontaneous protein degradation with rate γ. The noise of FPT is minimized using an optimal feedback strength α. A.** Protein accumulation for different feedback strategies *left*: $\alpha = -2\gamma$, *center*: $\alpha = \gamma$, *right*: $\alpha = 5\gamma$. *Top*: FPT histogram. *Bottom*: Some illustrative trajectories of protein level x as a function of time. **B.** The noise in FPT (measured by its coefficient of variation CV_T is plotted as a function of α . The analytical expression (25) is compared with CV_T values obtained by performing stochastic simulations (the line width shows the 95% confidence interval from 10,000 simulation replicas). The parameter values used for this graph are $\gamma = 1$, k_0 such that $\langle T\rangle \approx 1$, $x(0) = 0$, and $X = 100$.

IV. Optimal rates for linear self-regulation at low-noise regime

In this section, we consider the accumulation of biomolecular materials starting from $x(0) = 0$ with probability 1 and the degradation of molecules with rate γ. To simplify the feedback strategy, we assume a linear synthesis rate $k_i = k_0 + \alpha i$. Here, k_0 is the basal rate of protein production, and the slope α is called the feedback strength. In this case, positive feedback is implemented when $\alpha > 0$, and negative feedback occurs when $\alpha < 0$.

As a consequence of this linear stochastic formulation, the time evolution of the statistical moments of $x(t)$ can be obtained precisely by using the moment dynamics formalism.

$$\begin{aligned}\frac{d\langle x^m\rangle}{dt} &= \langle (k_0+\alpha x)\left[(x+1)^m - x^m\right] \\ &\quad +\gamma x\left[(x-1)^m - x^m\right]\rangle, \end{aligned} \tag{19}$$

for $m \in \{1, 2, \ldots\}$ [39]–[41]. Setting $m = 1$, the dynamics of the average copy number $\langle x\rangle$ is described by the following first-order system.

$$\frac{d\langle x\rangle}{dt} = k_0 + \alpha\langle x\rangle - \gamma\langle x\rangle \tag{20a}$$

$$\implies \langle x(t)\rangle = \frac{k_0(1 - e^{(-\gamma+\alpha)t})}{\gamma - \alpha}. \tag{20b}$$

In the limit of small fluctuations, the mean FPT $\langle T\rangle$ can be approximated by the time t at which $\langle x(t)\rangle = X$ yielding

$$\langle T\rangle \approx \frac{\ln\left[\frac{k_0}{k_0+(\alpha-\gamma)X}\right]}{\gamma - \alpha}. \tag{21}$$

Considering this linear feedback, while keeping $\langle T\rangle$ constant, we aim to find the optimal α that minimizes the noise in T. To fix $\langle T\rangle$ in the low-noise limit, we adjust k_0 according to α, from (21), as follows.

$$k_0 = \frac{(\alpha - \gamma)X}{e^{(\alpha-\gamma)\langle T\rangle} - 1}. \tag{22}$$

The variance in molecular counts is obtained analogously using $m = 2$ in (19),

$$\frac{d\langle x^2\rangle}{dt} = (k_0 + \alpha\langle x\rangle) + 2k_0\langle x\rangle + 2\alpha\langle x^2\rangle - 2\gamma\langle x^2\rangle + \gamma\langle x\rangle. \tag{23}$$

In this low-noise regime, the variance in FPT can be approximated as [42]

$$\sigma_T^2 \approx \lim_{t\to\langle T\rangle} \frac{\langle x^2\rangle - \langle x\rangle^2}{\left(\frac{d\langle x\rangle}{dt}\right)^2}, \tag{24}$$

and is inversely related to the slope at which the mean trajectory $\langle x\rangle$ approaches the threshold [42]. Hence, when this slope is *flatter*, the noise of threshold-hitting times is amplified. Plugging the solutions of (23) into (24) and using (20a)-(22), we obtain the following analytical expression for the coefficient of variation of T.

$$\begin{aligned} CV_T^2 &:= \frac{\sigma_T^2}{\langle T\rangle^2} \\ &\approx \frac{4\sinh^2[(\gamma-\alpha)\langle T\rangle/2](\gamma e^{(\gamma-\alpha)\langle T\rangle} - \alpha)}{(\gamma-\alpha)^3 X\langle T\rangle^2}. \end{aligned} \tag{25}$$

In the absence of degradation and assuming to have no feedback ($\gamma \to 0$ and $\alpha \to 0$), the formulas (21) and (25) reduce to the following exact forms

$$\langle T\rangle = \frac{X}{k_0}, \quad CV_T^2 = \frac{1}{X}, \tag{26}$$

respectively, which are consistent with (10) and (11).

Fig. 3 illustrates the effect of feedback strength α on CV_T^2, while keeping $\langle T\rangle$ constant by adjusting k_0 according to (22). The analytical approximation of CV_T^2 given by (25) matches well with the exact values from stochastic simulations, especially at low noise levels. As predicted, the discrepancy increases with higher noise. Moreover, CV_T^2 is a concave function of α with a global minimum. The optimal

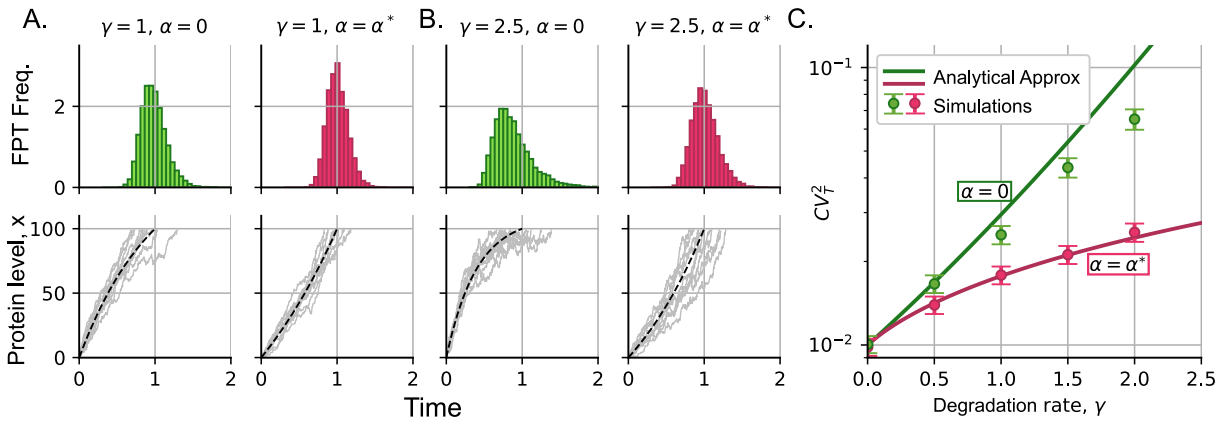

Fig. 3: **Stochastic variability in the FPTs monotonically increases with species degradation rate**. **A.** Illustrative examples of accumulation processes changing with degradation rate γ and the feedback strength α maintaining $\langle T\rangle = 1$. *Top*: FPT histogram. *Bottom*: Some illustrative trajectories of the protein level x as a function of time. **B.** Same as A. but with $\gamma = 2.5$. **C.** Noise in FPT measured by the squared coefficient of variation CV_T^2 versus γ keeping $\langle T\rangle$ fixed. Green represents the noise without feedback ($\alpha = 0$) and red represents the optimal linear feedback $\alpha = \alpha^*$ defined in (28)). The noise is calculated from the analytical expression (25), $x(0) = 0$, $X = 100$. Error bars represent the 95% confidence intervals of the simulation results using bootstrapping methods of 2000 replicas.

α, denoted by α^* which minimizes CV_T^2 is obtained by solving the equation:

$$\frac{d(CV_T^2)}{d\alpha} = 0. \tag{27}$$

Our analysis approximated the α^* as

$$\alpha^* \approx \gamma\left(1 + \frac{3}{1+3\gamma\langle T\rangle}\right). \tag{28}$$

This optimal solution implies positive feedback $\alpha^* > 0$ and depends on the dimensionless factor $\gamma\langle T\rangle$, which is the mean FPT normalized by the average protein lifespan $1/\gamma$. Fig. 3 compares the changes in CV_T^2 with γ for no feedback ($\alpha = 0$ in green) and optimal feedback ($\alpha = \alpha^*$ in red) with α^* as given by (28). As $\gamma \to 0$, we see that $\alpha^* \to 0$ and both lines converge to $CV_T^2 = 1/\langle X\rangle$, the fundamental lower bound of timing noise. For a fixed mean $\langle T\rangle$, the timing noise increases with γ, but more slowly for $\alpha = \alpha^*$ (red) than for $\alpha = 0$ (green).

V. Optimal feedback strategy for arbitrary synthesis rates

We now relax the assumption of a linear form to allow the synthesis rate to vary without restriction. Given the analytical intractability of this problem, we focus primarily our analysis on low threshold levels and zero initial conditions to get an idea of the optimal form of k_i. We first consider a threshold of $X = 2$ molecules where the optimization problem has an exact analytical solution.

A. *Threshold of two molecules*

The simplest system that includes protein degradation is presented in Fig. 4A consisting of the synthesizing of two molecules with life-span with mean $1/\gamma$. In this case, $X = 2$. Hence, we have to solve to two rates k_0 and k_1 that will minimize $\langle T^2\rangle$ for a fixed $\langle T\rangle$. To find the probability density function (pdf) of the first-passage time T we can write the Chemical Master Equation (CME) [43]–[46]

$$\frac{dP_0(t)}{dt} = -k_0 P_0(t) + \gamma P_1(t) \tag{29a}$$

$$\frac{dP_1(t)}{dt} = k_0 P_0(t) - \gamma P_1(t) - k_1 P_1(t), \tag{29b}$$

that describes the time evolution of the probabilities

$$P_i(t) := \mathbb{P}\{x(t) = i\},\ i \in \{0, 1\}. \tag{30}$$

Solving the linear dynamical system (29a) with initial conditions $P_0(0) = 1$ and $P_1(0) = 0$ gives the pdf of T which is defined as $f_T(t) = k_1 P_1(t)$. Using the obtained pdf, we find the following first- and second-order moments of T:

$$\langle T\rangle = \int_0^\infty t f_T(t)dt = \frac{\gamma + k_0 + k_1}{k_0 k_1} \tag{31a}$$

$$\langle T^2\rangle = \int_0^\infty t^2 f_T(t)dt = \frac{2\left((\gamma + k_0)^2 + (2\gamma + k_0)k_1 + k_1^2\right)}{k_0^2 k_1^2}. \tag{31b}$$

From (31a), a fixed $\langle T\rangle$ can be achieved by choosing:

$$k_0 = \frac{\gamma + k_1}{k_1\langle T\rangle - \gamma}. \tag{32}$$

The optimization is performed on k_1 that minimizes $\langle T^2\rangle$. The solution of this optimization reveals the optimal synthesis strategy to be

$$k_0 = k_1 = \frac{1 + \sqrt{1 + \gamma\langle T\rangle}}{\langle T\rangle}, \tag{33}$$

and the corresponding minimal FPT noise is

$$CV_T^2 = 1 - \frac{2}{2 + \gamma\langle T\rangle + 2\sqrt{1 + \gamma\langle T\rangle}}. \tag{34}$$

Fig. 4B illustrates the FPT distribution with rates chosen as (33) and illustrates its shape with increasing γ. Note that

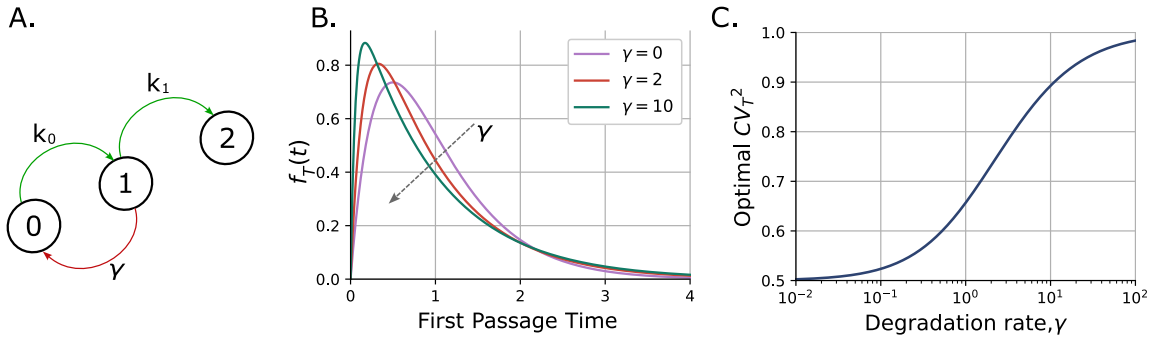

Fig. 4: **Optimal protein synthesis strategy for a threshold of two molecules considering a degradation rate** γ. **A.** Schematic diagram where, starting from zero proteins with the objective of reaching two molecules, we optimize the rates k_1 and k_0 such that we minimize the variability in the FPT T for fixed $\langle T\rangle$. **B.** The optimized FPT distribution $f_T(t)$ with miminial timing noise for different degradation rates γ. The optimal strategy corresponds to both rates being k_1 and k_0 equal and given by (33). **C.** Optimal timing variability as given by (34) as a function of γ. Here, $\langle T\rangle = 1$ and $x(0) = 0$ with probability one.

in the absence of degradation $\gamma = 0$, (34) reduces to $CV_T^2 = 1/X = 1/2$. For small values of $\gamma\langle T\rangle \ll 1$, the noise level can be approximated by $CV_T^2 \approx 1/2+\gamma\langle T\rangle/4$. Furthermore, CV_T^2 is a monotonically increasing function of $\gamma\langle T\rangle$, with $CV_T^2 \to 1$ at the limit $\gamma \to \infty$ (Fig. 4C). Recall that the CV of an exponential distribution is one, and this can be seen in the shape of $f_T(t)$ in Fig. 4B with $\gamma \to \infty$.

B. Threshold of five molecules

In our analysis, so far, we have found optimal strategies for some simplified cases. We derived the solution for protein accumulation without degradation, the low-noise solution for a high threshold, and the exact solution for a threshold of two molecules. However, we do not expect a simple analytical solution for the general case of protein accumulation with degradation and an arbitrary threshold. In this section, we resort to numerical methods to obtain the solution for the optimal form of k_i in a system with accumulation of five protein molecules, this is, $X = 5$.

To tackle this problem, we propose the general master equation:

$$\begin{cases} \dfrac{dP_0(t)}{dt} = -k_0 P_0(t) + \gamma P_1(t) \\ \dfrac{dP_i(t)}{dt} = k_{i-1}P_{i-1}(t) \\ \qquad\qquad - (k_i + \gamma i)\, P_i(t) + \gamma(i+1)P_{i+1}(t) \\ \vdots \\ \dfrac{dP_{X-1}(t)}{dt} = k_{X-2}P_{X-2}(t) \\ \qquad\qquad - (k_{X-1} + \gamma(X-1))\, P_{X-1}(t) \\ \dfrac{dP_X(t)}{dt} = k_{X-1}P_{X-1}(t), \end{cases} \tag{35}$$

which can be used to obtain the probability vector $\vec{P}(t) = [P_0(t), P_1(t), \cdots, P_{X-1}(t), P_X(t)]^\dagger$ at any time t. Each element $P_x(t)$ represents the probability of having x molecules at time t. In a more general notation, the system can be described by the matrix $\mathbf{A}$ such as:

$$\frac{d\vec{P}(t)}{dt} = \mathbf{A}\vec{P}(t), \tag{36}$$

which, given the initial conditions $P_x(t=0) = \delta_{x,0}$, with $\delta_{i,j}$ being the Kronecker delta distribution, can be solved using matrix exponential methods:

$$\vec{P}(t) = \exp(\mathbf{A}t)\vec{P}(t=0). \tag{37}$$

The moments of the FPT distribution can be estimated from the FPT pdf $f_T(t)$ which, using (35), follows:

$$f_T(t) = \frac{dP_X(t)}{dt} = k_{X-1}P_{X-1}(t). \tag{38}$$

We numerically solve the moments from the FPT distribution (38) and using brute-force search we find the set of k_i that minimizes the CV_T^2 for a fixed $\langle T\rangle$ with a level of accuracy of 0.01 on both variables. We considered three cases: no feedback (constant synthesis rates); linear feedback as in Section 4; and unconstrained feedback, where any arbitrary set of k_i is allowed.

Fig. 5 presents and contrasts these three different cases for $\gamma \in \{0, 1, 2\}$ with the normalized time, such that the mean FPT follows $\langle T\rangle = 1$. In the case without feedback (Fig. 5A), the constant rate is simply set by $\langle T\rangle$. In the particular case of $\gamma = 0$, these rates are given by (10). When the feedback is constrained to follow a linear function of the protein levels, we observe that the optimal slope is positive (positive feedback). Moreover, the slope of this relationship increases with γ, which is consistent with our earlier approximate analytical analysis. In Fig. 5C, where the rates are unconstrained, the optimal feedback involves first increasing the rates with protein numbers. These rates reach a maximum just before the threshold. Finally, the synthesis of the last molecule to reach the threshold can be done at a much lower rate. This implies that the optimal strategy here is mixed, positive feedback at the beginning and negative feedback close to threshold. A comparison of the three cases

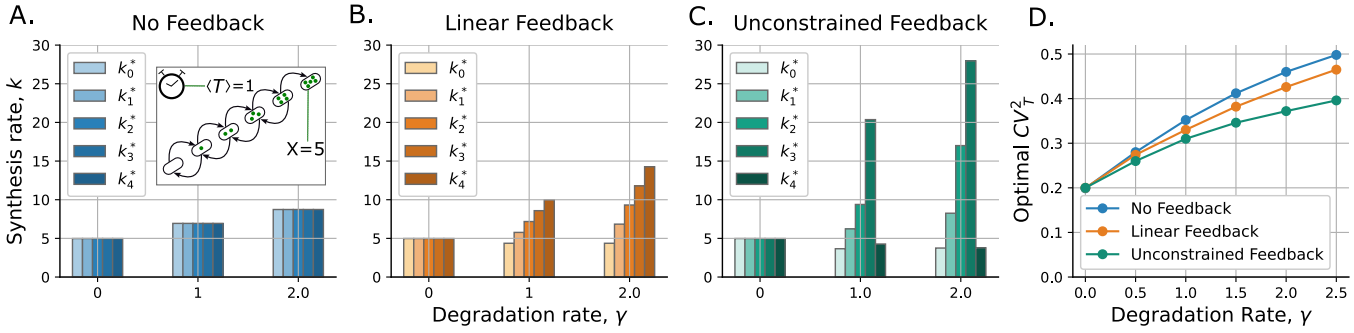

Fig. 5: **A mixture of positive and negative feedback leads to the lowest optimal noise in FPT when protein degradation is considered**. Optimal synthesis rates $\{k_0^*, k_1^*, ..., k_4^*\}$ for the threshold of five molecules starting with no molecules. **A.** Optimal rates considering a constant rate for all protein levels. (Inset: a diagram explaining the process of accumulation and degradation). **B.** In the case of linear feedback, the optimal synthesis rate increases with the protein level, consistent with our low noise limit analysis in Section IV. **C.** Considering unconstrained feedback, where any arbitrary set of k_i is allowed, results in a nonmonotonic form with first increasing synthesis rates, and then sudden decrease just before threshold. In the absence of degradation ($\gamma = 0$), the optimal synthesis rate is $k_i = X/\langle T \rangle$ regardless of the feedback strategy considered, as explained in Section III-A. **D.** Increasing the degradation rate γ , the accuracy of the timer decreases since the noise CV_T^2 in timing increases. A comparison of optimal noise in FPT for the three strategies. For this plot, $\langle T \rangle = 1$ and $x(0) = 0$ with probability one.

in Fig. 4D shows the additional noise suppression achieved as we relax the constraints on the synthesis rate.

VI. Conclusions

Accumulation of gene product levels is a key mechanism of biological timekeeping underlying diverse processes. For example, bacteriophages (viruses of bacterial cells) make proteins such as holin, that slowly build up in the host cell membrane, and the cell is lysed open upon holin's attaining a threshold level [47]–[49]. Experimental evidence points to viruses lysing cells around an optimal time to maximize fitness [50], thus motivating the problem we have considered. Timing of cell-cycle events, such as start of DNA replication and mitotic division into daughters is also strongly influenced by species levels reaching thresholds [51]–[57].

We reviewed previous results that when proteins are long-lived, the optimal accumulation strategy is to have a constant synthesis rate that minimizes noise in timing for a given fixed mean FPT [27]. In contrast, random initial conditions shift the strategy to negative feedback regulation with synthesis rates decreasing with increasing molecule counts. With protein degradation and forcing the feedback synthesis rate to have a linear form, we show that the optimal slope of the synthesis rate is positive and monotonically increases with γ (Fig 2). As one would expect, the accuracy of timing deteriorates with shortening protein half-lives, and in the limit of a highly unstable protein one cannot do better than timing approaching an exponentially-distributed random variable with $CV_T \to 1$ (Fig. 3).

Finally, we study numerically the global optimal synthesis strategy for a five-molecule accumulation. With increasing the degradation rate, we found a pattern in the dependence of optimal synthesis rates on protein levels. The optimal strategy consists of increasing the rate with protein levels until the last molecule synthesis. The accumulation rate of the final molecule should occur at a relatively low rate (Fig. 5). As part of the future work, we plan to use some of our intuition gained for small thresholds to build an analytical theory for any arbitrary threshold. Future work on this topic could also explore other sources of variability, such as noise from cell-cycle dependent factors [58], [59]. Moreover, it would be interesting to investigate how protein interactions with *decoys*, which can buffer protein copy number fluctuations [60], [61], affect timing variations.

References

[1] K. M. Schmoller, J. Turner, M. Kõivomägi, and J. M. Skotheim, "Dilution of the cell cycle inhibitor whi5 controls budding-yeast cell size," *Nature*, vol. 526, no. 7572, pp. 268–272, 2015.

[2] S. Patra and D. Chowdhury, "Level crossing statistics in a biologically motivated model of a long dynamic protrusion: passage times, random and extreme excursions," *Journal of Statistical Mechanics: Theory and Experiment*, vol. 2021, no. 8, p. 083207, 2021.

[3] C. R. Gliech and A. J. Holland, "Keeping track of time: the fundamentals of cellular clocks," *Journal of Cell Biology*, vol. 219, no. 11, 2020.

[4] J. Gerardin, N. R. Reddy, and W. A. Lim, "The design principles of biochemical timers: circuits that discriminate between transient and sustained stimulation," *Cell systems*, vol. 9, no. 3, pp. 297–308, 2019.

[5] J. Qian, L. Gelens, and M. Bollen, "Coordination of timers and sensors in cell signaling," *BioEssays*, vol. 41, no. 3, p. 1800217, 2019.

[6] M. Zhu, W. Chen, V. Mirabet, L. Hong, S. Bovio, S. Strauss, E. M. Schwarz, S. Tsugawa, Z. Wang, R. S. Smith, *et al.*, "Robust organ size requires robust timing of initiation orchestrated by focused auxin and cytokinin signalling," *Nature Plants*, pp. 1–13, 2020.

[7] C. Schwarz, A. Johnson, M. Kõivomägi, E. Zatulovskiy, C. J. Kravitz, A. Doncic, and J. M. Skotheim, "A precise Cdk activity threshold determines passage through the restriction point," *Molecular cell*, vol. 69, no. 2, pp. 253–264, 2018.

[8] Y. Goldschmidt, E. Yurkovsky, A. Reif, R. Rosner, A. Akiva, and I. Nachman, "Control of relative timing and stoichiometry by a master regulator," *PLOS ONE*, vol. 10, pp. 1–14, 2015.

[9] J. Roux, M. Hafner, S. Bandara, J. J. Sims, H. Hudson, D. Chai, and P. K. Sorger, "Fractional killing arises from cell-to-cell variability in overcoming a caspase activity threshold," *Molecular Systems Biology*, vol. 11, p. 803, 2015.

[10] A. L. Paek, J. C. Liu, A. Loewer, W. C. Forrester, and G. Lahav, "Cell-to-cell variation in p53 dynamics leads to fractional killing," *Cell*, vol. 165, no. 3, pp. 631–642, 2016.

[11] Y.-Y. Cheng, A. J. Hirning, K. Josic, and M. R. Bennett, "The timing of transcriptional regulation in synthetic gene circuits," *ACS synthetic biology*, vol. 6, no. 11, pp. 1996–2002, 2017.

[12] Z. Vahdat and A. Singh, "Frequency-dependent modulation of stochasticity in postsynaptic neuron firing times," in *2022 IEEE 61st Conference on Decision and Control (CDC)*, pp. 635–640, IEEE, 2022.

[13] K. Rijal, A. Prasad, and D. Das, "Protein hourglass: Exact first passage time distributions for protein thresholds," *Physical Review E*, vol. 102, no. 5, p. 052413, 2020.

[14] S. Gupta, S. Fancher, H. C. Korswagen, and A. Mugler, "Temporal precision of molecular events with regulation and feedback," *Physical Review E*, vol. 101, no. 6, p. 062420, 2020.

[15] K. Biswas, M. K. Jolly, and A. Ghosh, "First passage time properties of miRNA-mediated protein translation," *Journal of Theoretical Biology*, vol. 529, p. 110863, 2021.

[16] W. Y. C. Huang, S. Alvarez, Y. Kondo, J. Kuriyan, and J. T. Groves, "Relating cellular signaling timescales to single-molecule kinetics: A first-passage time analysis of Ras activation by SOS," *Proceedings of the National Academy of Sciences*, vol. 118, no. 45, 2021.

[17] K. Biswas and A. Ghosh, "First passage time in post-transcriptional regulation by multiple small rnas," *The European Physical Journal E*, vol. 44, no. 2, pp. 1–10, 2021.

[18] K. R. Ghusinga and A. Singh, "Optimal regulation of protein degradation to schedule cellular events with precision," in *2016 American Control Conference (ACC)*, pp. 424–429, IEEE, 2016.

[19] K. Rijal, A. Prasad, A. Singh, and D. Das, "Exact distribution of threshold crossing times for protein concentrations: Implication for biological timekeeping," *Physical Review Letters*, vol. 128, no. 4, p. 048101, 2022.

[20] O. Jouini and Y. Dallery, "Moments of first passage times in general birth–death processes," *Mathematical Methods of Operations Research*, vol. 68, pp. 49–76, 2008.

[21] L. Bondesson, "A characterization of first passage time distributions for random walks," *Stochastic Processes and their Applications*, vol. 39, pp. 81 – 88, 1991.

[22] M. R. D'Orsogna and T. Chou, "First passage and cooperativity of queuing kinetics," *Physical Review Letters*, vol. 95, p. 170603, 2005.

[23] C. Lo and T. Chung, "First passage time problem for the Ornstein-Uhlenbeck neuronal model," in *Neural Information Processing*, pp. 1155–1164, 2006.

[24] W. Dai, A. M. Sengupta, and R. M. Levy, "First passage times, lifetimes, and relaxation times of unfolded proteins," *Physical Review Letters*, vol. 115, p. 048101, 2015.

[25] A. Szabo, K. Schulten, and Z. Schulten, "First passage time approach to diffusion controlled reactions," *The Journal of Chemical Physics*, vol. 72, pp. 4350–4357, 1980.

[26] Z. Vahdat, K. R. Ghusinga, and A. Singh, "Comparing feedback strategies for minimizing noise in gene expression event timing," in *2021 29th Mediterranean Conference on Control and Automation (MED)*, pp. 450–455, IEEE, 2021.

[27] K. R. Ghusinga, J. J. Dennehy, and A. Singh, "First-passage time approach to controlling noise in the timing of intracellular events," *Proceedings of the National Academy of Sciences*, vol. 114, pp. 693–698, 2017.

[28] C. Nieto, K. R. Ghusinga, and A. Singh, "Feedback strategies for threshold crossing of protein levels at a prescribed time," in *2022 30th Mediterranean Conference on Control and Automation (MED)*, pp. 170–175, IEEE, 2022.

[29] A. Singh, B. Razooky, C. D. Cox, M. L. Simpson, and L. S. Weinberger, "Transcriptional bursting from the HIV-1 promoter is a significant source of stochastic noise in HIV-1 gene expression," *Biophysical journal*, vol. 98, pp. L32–L34, 2010.

[30] N. Molina, D. M. Suter, R. Cannavo, B. Zoller, I. Gotic, and F. Naef, "Stimulus-induced modulation of transcriptional bursting in a single mammalian gene," *Proceedings of the National Academy of Sciences*, vol. 110, pp. 20563–20568, 2013.

[31] N. Kumar, A. Singh, and R. V. Kulkarni, "Transcriptional bursting in gene expression: analytical results for general stochastic models," *PLoS computational biology*, vol. 11, no. 10, p. e1004292, 2015.

[32] A. M. Corrigan, E. Tunnacliffe, D. Cannon, and J. R. Chubb, "A continuum model of transcriptional bursting," *eLife*, vol. 5, p. e13051, 2016.

[33] D. M. Suter, N. Molina, D. Gatfield, K. Schneider, U. Schibler, and F. Naef, "Mammalian genes are transcribed with widely different bursting kinetics," *Science*, vol. 332, pp. 472–474, 2011.

[34] A. Raj, C. Peskin, D. Tranchina, D. Vargas, and S. Tyagi, "Stochastic mRNA synthesis in mammalian cells," *PLOS Biology*, vol. 4, p. e309, 2006.

[35] V. Shahrezaei and P. S. Swain, "Analytical distributions for stochastic gene expression," *Proceedings of the National Academy of Sciences*, vol. 105, pp. 17256–17261, 2008.

[36] A. J. Larsson, P. Johnsson, M. Hagemann-Jensen, L. Hartmanis, O. R. Faridani, B. Reinius, Å. Segerstolpe, C. M. Rivera, B. Ren, and R. Sandberg, "Genomic encoding of transcriptional burst kinetics," *Nature*, vol. 565, no. 7738, pp. 251–254, 2019.

[37] K. Ghusinga and A. Singh, "Theoretical predictions on the first-passage time for a gene expression model," *IEEE Conf. on Decision and Control, Osaka, Japan*, pp. 3864–3869, 2015.

[38] K. R. Ghusinga and A. Singh, "Effect of gene-expression bursts on stochastic timing of cellular events," in *2017 American Control Conference (ACC)*, pp. 2118–2123, IEEE, 2017.

[39] J. P. Hespanha and A. Singh, "Stochastic models for chemically reacting systems using polynomial stochastic hybrid systems," *International Journal of Robust and Nonlinear Control*, vol. 15, pp. 669–689, 2005.

[40] A. Singh and J. P. Hespanha, "Approximate moment dynamics for chemically reacting systems," *IEEE Transactions on Automatic Control*, vol. 56, pp. 414–418, 2011.

[41] A. Singh and J. P. Hespanha, "Stochastic hybrid systems for studying biochemical processes," *Philosophical Transactions of the Royal Society A*, vol. 368, pp. 4995–5011, 2010.

[42] M. C. Lagomarsino, M. Caselle, M. Osella, *et al.*, "Stochastic timing in gene expression for simple regulatory strategies," *Nucleic Acids Research*, p. gkw1235, 2016.

[43] D. T. Gillespie, "A general method for numerically simulating the stochastic time evolution of coupled chemical reactions," *Journal of Computational Physics*, vol. 22, pp. 403–434, 1976.

[44] D. A. McQuarrie, "Stochastic approach to chemical kinetics," *Journal of applied probability*, vol. 4, pp. 413–478, 1967.

[45] D. J. Wilkinson, *Stochastic Modelling for Systems Biology*. Chapman and Hall/CRC, 2011.

[46] D. J. Wilkinson, "Stochastic modelling for quantitative description of heterogeneous biological systems," *Nature Reviews Genetics*, vol. 10, pp. 122–133, 2009.

[47] C.-Y. Chang, K. Nam, and R. Young, "S gene expression and the timing of lysis by bacteriophage lambda," *Journal of Bacteriology*, vol. 177, pp. 3283–3294, 1995.

[48] A. Singh and J. J. Dennehy, "Stochastic holin expression can account for lysis time variation in the bacteriophage λ," *Journal of the Royal Society Interface*, vol. 11, p. 20140140, 2014.

[49] J. J. Dennehy and I.-N. Wang, "Factors influencing lysis time stochasticity in bacteriophage λ," *BMC Microbiology*, vol. 11, p. 174, 2011.

[50] S. Kannoly, T. Gao, S. Dey, N. Wang, A. Singh, and J. J. Dennehy, "Optimum threshold minimizes noise in timing of intracellular events," *iScience*, vol. 23, p. 101186, 2020.

[51] K. R. Ghusinga, C. A. Vargas-Garcia, and A. Singh, "A mechanistic stochastic framework for regulating bacterial cell division," *Scientific Reports*, vol. 6, 2016.

[52] F. Si, G. Le Treut, J. T. Sauls, S. Vadia, P. A. Levin, and S. Jun, "Mechanistic origin of cell-size control and homeostasis in bacteria," *Current Biology*, vol. 29, no. 11, pp. 1760–1770, 2019.

[53] R. Tsukanov, G. Reshes, G. Carmon, E. Fischer-Friedrich, N. S. Gov, I. Fishov, and M. Feingold, "Timing of z-ring localization in escherichia coli," *Physical Biology*, vol. 8, p. 066003, 2011.

[54] G. Reshes, S. Vanounou, I. Fishov, and M. Feingold, "Timing the start of division in e. coli: a single-cell study," *Physical Biology*, vol. 5, p. 046001, 2008.

[55] A. Amir, O. Kobiler, A. Rokney, A. B. Oppenheim, and J. Stavans, "Noise in timing and precision of gene activities in a genetic cascade," *Molecular Systems Biology*, vol. 3, p. 71, 2007.

[56] E. Yurkovsky and I. Nachman, "Event timing at the single–cell level," *Briefings in Functional Genomics*, vol. 12, pp. 90–98, 2013.

[57] J. M. Bean, E. D. Siggia, and F. R. Cross, "Coherence and timing of cell cycle start examined at single-cell resolution," *Molecular Cell*, vol. 21, pp. 3–14, 2006.

[58] Z. Vahdat, Z. Xu, and A. Singh, "Modeling protein concentrations in cycling cells using stochastic hybrid systems," *IFAC-PapersOnLine*, vol. 54, no. 9, pp. 521–526, 2021.

[59] C. Cadart, L. Venkova, M. Piel, and M. C. Lagomarsino, "Volume growth in animal cells is cell cycle dependent and shows additive fluctuations," *Elife*, vol. 11, p. e70816, 2022.

[60] S. Dey, M. Soltani, and A. Singh, "Enhancement of gene expression noise from transcription factor binding to genomic decoy sites," *Scientific reports*, vol. 10, no. 1, pp. 1–13, 2020.

[61] A. Burger, A. M. Walczak, and P. G. Wolynes, "Influence of decoys on the noise and dynamics of gene expression," *Physical Review E*, vol. 86, p. 041920, 2012.